Real-Time Virtual Surgery Simulation Employing MM-Model and Adaptive Spatial Hash

Shaoting Zhang[1], Lixu Gu[1], Weiming Liang[2], Jingsi Zhang[1], and Feng Qian[2]

[1] School of Software, Shanghai Jiao Tong University
http://www.se.sjtu.edu.cn/igst/~stzhang.htm
[2] ACM Class, Shanghai Jiao Tong University

Abstract. In this paper, MM-Model is presented for real-time simulation of 3D deformable objects on both global level and local region. This model consists of a deformable centerline and dynamic surface reconstruction mechanism based on Mass-Spring and Medial-Representation respectively. When a relatively small force is applied on the object the model works in the same way as the traditional Mass-Spring. Otherwise the force is directly transferred to the centerline and the surface is dynamically recreated according to the position of the centerline. This model works more effectively and efficiently than traditional elastic ones on the global level due to the advantages of the Medial-Representation reflecting the internal information and the Mass-Spring reducing the response time. A novel collision detection algorithm based on adaptive spatial hash, a cutting approach and suture method are also articulated. An artificial blood vessel's deformation effect and surgery processes are presented in our case study.

1 Introduction

Real-time simulation of deformable objects becomes increasingly important in Virtual Reality, especially in the virtual surgery. More and more inexperienced surgeons and students begin to use this technology instead of practicing on cadavers. However, immediately and accurately modeling as well as interaction has still been the bottleneck.

Various models have been proposed to simulate soft tissue and other deformable objects. Finite Element Method (FEM) is famous for accuracy when simulating local deformation [1], but it is time-consuming and difficult to implement. Mass-Spring systems are fast when the number of nodes is relatively small [2], while they are not very accurate and its stability depends on the value of parameters. Chain-Mail satisfies the real-time requirement but it does not reflect the real physical characteristics of these objects [3]. In addition, these models focus on local area deformation, such as cutting, pressing and nipping. All of them might not be suitable for simulating global deformation due to the following problems: (1) the elastic model is inappropriate for simulating global

Z. Pan et al. (Eds.): ICAT 2006, LNCS 4282, pp. 666–675, 2006.

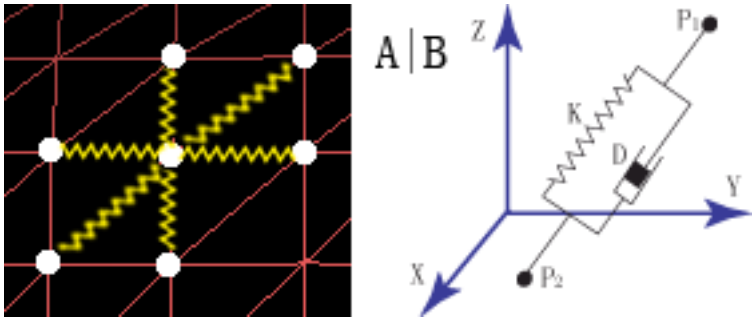

Fig. 1. (A) The topology of mass points and springs; (B) The basic component of Mass-Spring system (D = damper)

deformation because of the unacceptable distortion; (2) global motion requires much more calculation time than local movement [4]; (3) the inner structure is not well presented.

In this paper, we want to solve the problems mentioned above and propose a novel MM-Model. A deformable centerline based on a Mass-Spring system and a Medial Representation model is combined to simulate both large and small scale motion [5]. If external force is applied on a local region, the model works as a pure surface Mass-Spring system; otherwise, the force will be directly applied to the centerline and the surface will be reconstructed according to the position of the moving centerline. Additionally, we advance a multi-resolution hashing algorithm for the real-time collision detection between deformable objects and established a surgery-training system on an artificial blood vessel with cutting and suture simulation.

The following sections describe the hybrid model and collision detection algorithm in detail. In section 2 we introduce the method to model the deformable centerline, Medial Representation modeling and surface-reconstruction mechanism, all of which lead to the MM-Model. In section 3 some virtual reality algorithms such as collision detection, collision response, cutting and suture are presented. Finally, we present the experiment results in section 4.

2 MM-Model

2.1 Deformable Centerline Modeling

Mass-Spring models the non-rigid object as a collection of mass points linked by springs and dampers in a mesh structure. The topology of the mass points and springs on the surface is described in Fig. 1(A), and Fig. 1(B) displays the compositions of the basic unit of the system: the elastic spring and the damper. The former engenders the elasticity force proportional to the springs length change, and the latter generates damping force relative to the velocity of points.

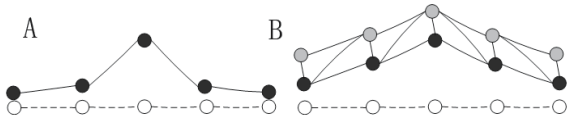

Fig. 2. Apply a force on the middle-point of the centerline. (A) A crest appears on the centerline with the linear topology (The write dots = the initial position of centerline; The black dots = the position after deformation; the black lines = springs); (B) A smooth effect of the centerline with DALs (The grey dots = Virtual atoms).

The Mass-Spring system employs a differential equation to calculate the coordinates of mass points:

$$m_i \cdot \frac{\partial^2 \boldsymbol{x_i}}{\partial t^2} + d_i \cdot \frac{\partial \boldsymbol{x_i}}{\partial t} + \sum_{j \in \sigma(i)} k_{i,j} \cdot \delta l_{i,j} = F_i \ . \tag{1}$$

Where m_i, d_i, and F_i are the mass, damping factor and external force of the ith mass respectively. x_i is the $3n$ vector displacement of the ith mass points. σ_i represents the mass points directly linked to the ith mass. $k_{i,j}$ and $\delta l_{i,j}$ denotes the elasticity factor and the length alternation of spring ij respectively. The mass-spring system is employed to model the surface mesh and the deformable centerline.

The Distance Mapping Method is employed to extract the centerline [7], along which media atoms are selected evenly and automatically. The density of the atoms determines the resolution of the surface mesh. After the extraction, the centerline is modeled as a Mass-Spring system: the atoms are considered as mass points and linked with springs.

However, the propagation of the force applied on this linear elastic model is not simultaneous due to the linear layout of the centerline. Therefore, an unreasonable crest will occur in a local area (Fig. 2(A)). To solve the problem, some optimizations are realized. A Dynamic-Assistant-Line (DAL) is created to construct a layered topology (Fig. 2(B)). Virtual atoms and DALs (dash lines) are generated parallel to the centerline and vertical to the external force, and this layered Mass-Spring system can accelerate the propagation of the force, which could ameliorate the crest-problem.

Additionally, an Angular Spring (AS) and Return Spring (RS) are designed to refine the deformation appearance [8][9]. The former is used to simulate the curvature force which controls the bending degree; the latter is utilized to prevent the model from escaping from the initial position.

2.2 Medial Representation Modeling

After the construction of the centerline model, the Medial Representation model used to dynamically obtain the surface information needs to be created.

Stephen M. Pizer presented the M-Rep theory, a type of Medial Representation, based on Blums medial axes [10]. This model uses medial atoms (Fig. 3(A))

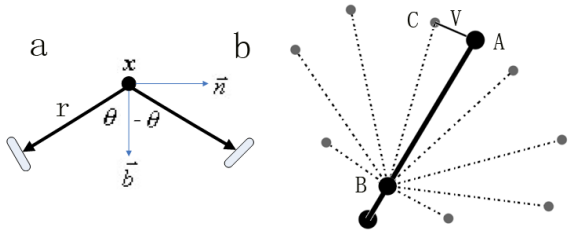

Fig. 3. (A) M-Rep topology in 3D; (B) 3D simplified Medial Representation in stable position (A, B = medial atoms; C = implied boundary; $\boldsymbol{V}$ = Orientation Vector)

to represent the interior section and a particular tuple ($\{x, r, F(\boldsymbol{b}, \boldsymbol{n}), \theta\}$) to imply the boundary position [5]. M-Rep is widely used in the fields of segmentation but it is not suitable for simulation modeling due to the expensive calculation cost. Thus we redefine the topology of medial atoms just like hub-and-spoke (Fig. 3(B)). The corresponding tuple is altered to $\{x, r, F(\boldsymbol{V}, \boldsymbol{AB}), \theta\}$, where x is the 3D coordinates of the medial atom B; r is the length of the spoke $\boldsymbol{BC}$; $F(\boldsymbol{V}, \boldsymbol{AB})$ is the plane determined by $\boldsymbol{V}$ and centerline $\boldsymbol{AB}$; $\boldsymbol{V}$ is the Orientation Vector of boundary C, which links A with C; θ is the angle between $\boldsymbol{AB}$ and $\boldsymbol{BC}$.

The Basic Reconstruction Mechanism. As described in Section2.1 the centerline will move under the global level external force. Here we only simulate the elasticity force and curvature force, but excluding the constraint force, in order to realize the dynamically surface reconstructing. Therefore the movement of the centerline is limited to translation and rotation around the medial atoms but no spin around. Thus the coordinates of boundary C can be dynamically and uniquely determined by the following formula:

$$\underline{C} = x + R_{\boldsymbol{V},\boldsymbol{AB}}(\theta)\boldsymbol{AB} \cdot r_{\boldsymbol{BC}}/|\boldsymbol{AB}| \ . \tag{2}$$

Where $\underline{C}$ and x is the coordinates of boundary C and medial atom B respectively; R denotes the operator to rotate its operand by the argument angle in the plane spanned by $\boldsymbol{V}$ and $\boldsymbol{AB}$; $|\boldsymbol{AB}|$ means the length of the vector $\boldsymbol{AB}$. Other spokes connecting with B can be calculated by rotating $\boldsymbol{BC}$ around $\boldsymbol{BA}$ and scale the r length. Iterating the process can obtain all boundaries [11].

The Advanced Reconstruction Mechanism. The reconstruction mechanism mentioned in the above suffers two drawbacks: (1) If the value of θ is a constant during the deformation, the position of the reconstructed surface points might be inappropriate because the included angle of the centerline's subsections will be changed (Fig. 4(B)); (2) The neighboring spokes might intersect with each other if the centerline bends too much. Both of the problems might deteriorate the appearance of soft tissue (Fig. 4(B)).

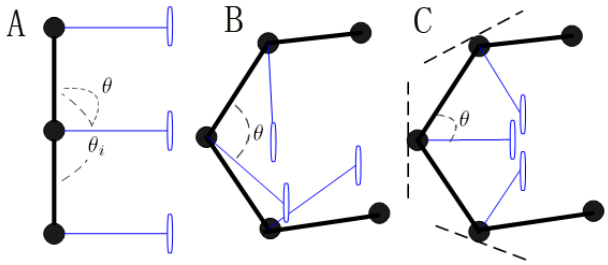

Fig. 4. (A) The initial layout of centerline and spokes (Black dots = medial atoms; blue ellipses = implied boundaries; the bold black line = centerline; thin blue lines = spokes); (B) The irregular topology of spokes according to the basic reconstruction mechanism; (C) The ideal arrangement of spokes according to the advanced reconstruction mechanism (dash lines = tangents)

The first problem is solved by defining a constant degree-ratio λ, which is expressed as the quotient of the initial θ devided by the corresponding initial included angle θ_i. When the centerline is moving, the value of θ is calculated by multiplying the constant λ with the variant θ_i, then tangents are created for spokes to rotate instead of the centerline's subsections. This strategy ensures a reasonable magnitutde for θ during the deformation (Fig. 4(C)).

To conquer the second drawback we rearrange all the intersecting spokes to reasonable positions according to the following algorithm: all of the intersected spokes are discarded except the first one (marked as $\boldsymbol{V}_1$) until we find the first uncrossed spoke (marked as $\boldsymbol{V}_2$); then the discarded spokes will be inserted into the the equally divided positions between $\boldsymbol{V}_1$ and $\boldsymbol{V}_2$. The two adjustments ensure a reasonable arrangement of all the spokes and polish the appearance of the deformable objects.

The deformation algorithm is switched between the surface mass-spring model and the reconstruction model according to the magnitude of the external force: if the force is larger than the pre-defined threshold, it will be directly transfered to the nearest three media atoms and the position of the surface will be recalculated based on the advanced reconstruction mechanism; otherwise the mass-spring model will be employed to describe the deformation.

3 Virtual Reality

3.1 Collision Detection

Collision detection algorithm is used to determine if and when geometric objects intersect. Physically based modeling simulations depend highly on the physical intersection between objects in a scene. Complex physics engines require fast, accurate, and robust proximity queries to maintain a realistic simulation at interactive rates. Generally, collision-detection algorithms has to deal with two

important phases, broad-phase and narrow-phase collision detection. The former one could efficiently determine all potential collision pairs in a scene with n objects, and the latter one checks potentially colliding pairs by applying an primitive intersection test. The problem of collision detection for static environments can be regarded as already solved. Generally, in a preprocessing step, an accelerating data structure is computed, and then, this data structure is used for optimally efficient borad and narrow phase collision detection. if the force is smaller than the threshold. However, the problem is more difficult when dealing with deformable models because such objects might change their shape each simulation step, which means that the accelerating data structure needs to be recomputed at runtime. Moreover, traditional uniform spatial partitioning approach is unsuitable for deformable objects, since the size of primitive (eg: tetrahedrons) will be changed during the deformation, which might make the pre-defined grid-resolution too high or too low. The high resolution means one primitive occupies a lot of grid-cells and the mapping process becomes extremely costly which the check for collisions in the case is very exact and fast, and the low resolution means many primitives are mapped into one single grid-cell, broad-phase collision detection works not very effective which leads to high costs in the narrow-phase since many primitives have to be checked for intersection.

In our approach, we advance an adaptive multi-resolution spatial partitioning algorithm [12] to devide the space and a hash table to store the position information of the deformable objects. Such approach could conquer the uniform-grid problems and achieve an efficient collision detection result.

In the partitioning stage, an optimal cell-size for each tetrahedron needs to be able to find. The assumption is that an optimal cell-size is given when a tetrahedron is mapped into less than eight cells and more than four cells. In the mapping stage, an unique address needs to be found for each possible grid cell. In the hashing stage, the hash function which is efficiently computable and good distribution is chosen to map grid-cells uniformly over the whole hash table.

Thus the previously introduced stages are combined to form the adaptive multi-resolution spatial hashing algorithm. Firstly, assuming a scene consisting of m tetrahedrons. For each tetrahedron the grid-cells that it occupies are computed. A reference to the tetrahedron is hashed into all occupied grid-cells. Secondly, for each vertex in the scene, it is computed which grid-cell it occupies. The vertex has to be tested for intersection with all tetrahedrons that also occupy that grid-cell. Doing those processes in every simulation steps, the collision detection effect is achieved. In the application, the update rate is more than 50 times per second when the collision detection algorithm is employed between two deformable objects each consists of 49848 tetrahedrons, which satisfy the real-time requirement.

3.2 Cutting and Suture

Cutting. A typical approach of cutting is described as the following steps: (1) Constantly collision detecting between the deformable object and the surgery equipment. (2) When the collision is detected, collision response will be invoked

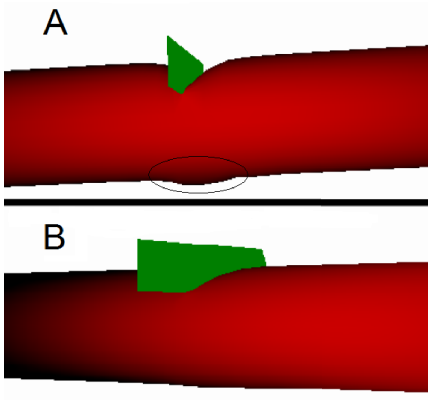

Fig. 5. Comparison between typical cutting method and centerline approach. (A) The force is transferred to the centerline and get a global deformation; (B) The force affects the local region.

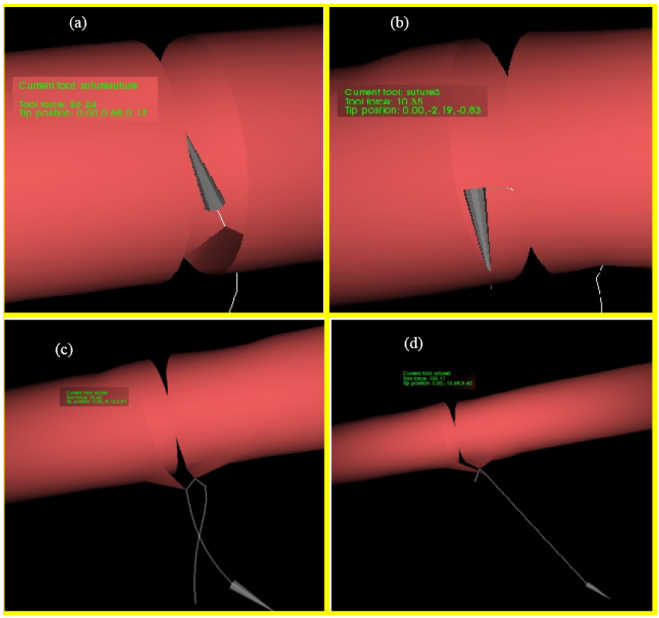

Fig. 6. Simulation of the suture process using FTL algorithm

and the soft object will deformed according to the external force. (3) If the internal force is larger than the pre-defined threshold, the spings will be cut, which means the corresponding triangles or tetrahedrons will be removed, and then the points connected by these springs will move back to the balanced position. (4) A friction force will be appended between the surgery equipment and the deformable object in order to obtain a more realistic simulation effect.

However, this algorithm does not take the global deformation into consideration, which result in the unreasonable effect in the global level. In our approach, part of the external force will be transferred to the centerline structure through spokes, and this force could ensure a global deformation result Fig. 5 (A),(B).

Suture. Follow The Leader (FTL) [13] algorithm is employed in the suture simulation. The algorithm is described here: (1) Define a line to represent the needle and stitches and evenly select 50 points on the line. Assume that the needle and the stitch between two neighbouring points are rigid objects, which means that the length between two points is constant. (2) Add the first point P_0 to the array of Control Points. (3) Move P_0 to a new position P_0'. The moving vector is $\boldsymbol{P_0P_0'}$. (4) Move the second point P_1 along the direction $\boldsymbol{P_1P_0} - \boldsymbol{P_0P_0'}$ until the distance between P_1 and P_0' is $|\boldsymbol{P_1P_0}|$, which is the original length of this stitch. (5) Add the second point P_1' to the array of Control Points and iterate the above processes until all points are moved to the next position. Fig. 6 displays the result of suture simulation.

4 Experiments

The tests are performed on a computer with an Intel Pentium IV-2.80 GHz CPU, 1.0 G bytes of DDR2 memory and a GeForce 6800 graphics card. The code is compiled with Visual C++ 7.0. The model is a part of an artifact blood vessel. There are 1142 points on the surface and 2280 polygons in the structure.

Fig. 7 compares the global deformation appearance of the hybrid model with both the surface and volume elastic models. Fig. 7(A) and Fig. 7(B) are the solid and mesh view of the Hybrid Model under the global-level force based on the advanced reconstruction mechanism; Fig. 7(C) is the result of the volume Mass-Spring model under large scale forces (the volume mesh contains 3564 points

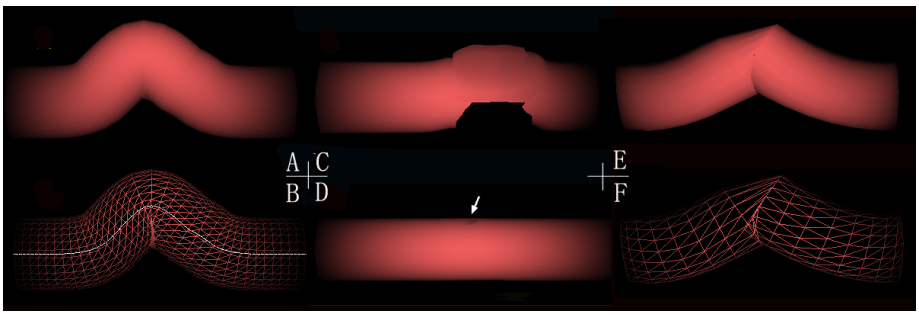

Fig. 7. Deformation effect of the artifact blood vessel (A) Global deformation of the Hybrid Model based on the advanced reconstruction mechanism; (B) Mesh view of (A) with the centerline; (C) Global deformation of the volume Mass-Spring model; (D) Local Deformation of the Hybrid Model (the same as the Surface Mass-Spring model); (E) Global deformation of the Hybrid Model using the basic reconstruction mechanism; (F) Mesh view of (E)

(1142 on the surface) and 17887 voxels). Fig. 7(D) is the local deformation effect of the hybrid model, which is the same as the surface mass-spring model. Fig. 7(E) and Fig. 7(F) display the appearance of the hybrid model using the basic reconstruction mechanism.

Table 1. Comparison of the calculation time between different models (milliseconds per update time, the calculation time = the time used for computing the displacements). (LF = local force; GF = global force; 10, 20, 100, 200, 400 = the magnitude of the forces).

	Surface Mass-Spring	Volume Mass-Spring	Mass-Spring + M-Rep
LF(10)	1.281	6.437	1.266
LF(20)	1.265	6.422	1.375
GF(100)	1.406	7.282	0.455
GF(200)	1.657	9.297	0.470
GF(400)	2.093	15.281	0.541

Table. 1 displays the computation time of different models. Here local force means that we apply a relatively small force (less than 50 units) on a surface point, and global force means that a large force (more than 100) is applied on 10 points. The update rate (including the rendering time) of the hybrid model is about 300 times, such rate is more efficient than the volume mass-spring model and meets with the real-time requirement (15-20 times per second). Additionally, the response time of the hybrid model will not be increased with the scale of the external force since the time complexity of the reconstruction mechanism depends on the whole number of spokes, while the mass-spring model does not have the advantadge because the computation time of the elastic formula 1 depends on the springs involved in the calculation.

5 Conclusions and Future Work

In this paper, we proposed a MM-Model based on Mass-Spring systems and Medial Representation to simulate deformable objects and adaptive spatial hash for real-time collision detection between deformable objects. The superior feature of the model is the effective and efficient simulation of global level deformation. Our main contribution is simplifying M-Rep and combining it with Mass-Spring systems. However, this model is unsuitable for bodies with complex surface structure, such as the heart, because the dynamical reconstruction mechanism cannot reasonably deal with lots of centerline branches.

In the future, we want to improve our approach and model more complex soft tissue. Moreover, the topology of the centerline needs to be optimized in order to obtain a more reasonable effect. Our current goal is to establish a clinical training system.

Acknowledgements

This work was partially supported by the Natural Science Foundation of China, grant NO. 70581171, and the Shanghai Municipal Research Fund, grant NO. 045118045. The author would like to thank Prof. Pizer for bringing the concept of M-Rep to our lab and discussing with us patiently. We also thank Shanghai Ren Ji Hospital for the experts' opinion.

References

1. Cotin, S., Delingette, H., and Ayache, N.: Real-time Elastic Deformations of Soft Tissues for Surgery Simulation. IEEE Transactions on Visualization and Computer Graphics. VOL. 5, NO. 1, pp. 72-83, January-March, 1999
2. Frisken, S.: Using Linked Volumes to Model Object Collisions, Deformation, Cutting, Carving, and Joining. IEEE Transactions on Visualization and Computer Graphics. VOL. 5, NO. 4, pp. 333-349, October-December, 1999
3. Sarah, F., Delingette, H., and Ayache, N.: A Fast Algorithm for Deforming Volumetric Objects. 1997 Symposium on Interactive 3D Graphics. pp. 149-154, April 1997
4. Zhuang, Y.: Real-time and Physically Realistic Simulation of Global Deformation. ACM SIGGRAPH 99 Conference. pp. 270, 1999
5. Pizer, S.: Multiscale Medial Loci and Their Properties. IJCV Special UNC-MIDAG issue. VOL. 55(2/3), pp. 155-179, 2003
6. Chen, Y., Zhu, Q., and Kaufman, A.: Physically-based Animation of Volumetric Objects. Computer Animation 1998.
7. Jiang, X., Gu, L.: An Automatic and Fast Centerline Extraction Algorithm for Virtual Colonoscopy. Engineering in Medicine and Biology Conference 2005.
8. Nedel, L., Thalmann, D.: Real Time Muscle Deformations Using Mass-Spring Systems. Proceedings of the Computer Graphics International. pp. 156-166, 1998
9. Zhang, S., Gu, L.: Real-Time Simulation of Deformable Soft Tissue Based on Mass-Spring and Medial Representation. CVBIA, LNCS 3875. pp. 421-428, 2005
10. Blum, Shape Description Using Weighted Symmetric Axis Features. Pattern Recognition. VOL. 10, pp. 167-180, 1978
11. Huang, P., Gu, L., and Zhang, S.: Real-Time Simulation for Global Deformation of Soft-Tissue Using Deformable Centerline and Medial Representation. ISBMS'06, LNCS 4072. pp 67-74, 2006
12. Eitz, M.: Realtime Soft Tissue Simulation employing Constraint Based Particle Systems and Hierarchical Spatial Hashing. Master Thesis of Shanghai Jiao Tong University. 2006
13. Brown, J., Sorkin, S., and Stephanides, M.: Algorithmic Tools for Real-Time Microsurgery simulation. Medical Image Analysis. 2002